Wave Reflection from Partially-Perforated-Wall Caisson Breakwater

Kyung-Duck Suh[a,*], Jae Kil Park[b], Woo Sun Park[c]

[a]*School of Civil, Urban, and Geosystem Engineering, Seoul National University, San 56-1, Shillim-Dong, Gwanak-Gu, Seoul 151-742, Republic of Korea*
[b]*Daelim Industrial Co., Ltd., 146-12, Susong-Dong, Jongno-Gu, Seoul 110-732, Republic of Korea; formerly graduate student at Seoul National University*
[c]*Coastal and Harbor Engineering Research Division, Korea Ocean Research and Development Institute, Ansan P.O. Box 29, 425-600, Republic of Korea*

Abstract: In 1995, Suh and Park developed a numerical model that computes the reflection of regular waves from a fully-perforated-wall caisson breakwater. This paper describes how to apply this model to a partially-perforated-wall caisson and irregular waves. To examine the performance of the model, existing experimental data are used for regular waves, while a laboratory experiment is conducted in this study for irregular waves. The numerical model based on a linear wave theory tends to over-predict the reflection coefficient of regular waves as the wave nonlinearity increases, but such an over-prediction is not observed in the case of irregular waves. For both regular and irregular waves, the numerical model slightly over- and under-predicts the reflection coefficients at larger and smaller values, respectively, because the model neglects the evanescent waves near the breakwater.

Keywords: Breakwaters; Laboratory tests; Numerical models; Perforated-wall caisson; Water waves; Wave reflection

* Corresponding author. Fax: +82-2-887-0349. *E-mail addresses*: kdsuh@snu.ac.kr (K.-D. Suh), roadpark@dic.co.kr (J. K. Park), wspark@kordi.re.kr (W. S. Park)

1. Introduction

A perforated-wall caisson breakwater is often used to remedy the drawbacks of a vertical caisson breakwater. It reduces not only wave reflection but also wave transmission due to overtopping. It also reduces wave forces, especially impulsive wave forces, acting on the caisson (Takahashi and Shimosako, 1994; Takahashi et al., 1994). A conventional perforated-wall caisson consists of a front wave chamber and a back wall as shown in Fig. 1(a), and the water depth inside the wave chamber is the same as that on the rubble foundation. The weight of the caisson is less than that of a vertical solid caisson with the same width, and moreover most of this weight is concentrated on the rear side of the caisson. Therefore, difficulties are sometimes met in the design of a perforated-wall caisson to satisfy the design criteria against sliding and overturning. In addition, particularly in the case where the bearing capacity of the seabed is not large enough, the excessive weight on the rear side of the caisson may have an adverse effect. In order to solve these problems, a partially-perforated-wall caisson as shown in Fig. 1(b) is often used, which provides an additional weight to the front side of the caisson. In this case, however, other hydraulic performance characteristics of the caisson such as wave reflection and overtopping may become worse compared with a fully-perforated-wall caisson.

In order to examine the reflection characteristics of a perforated-wall caisson breakwater, hydraulic model tests have been used (Jarlan, 1961; Marks and Jarlan, 1968; Terret et al., 1968; Bennett et al., 1992; Park et al., 1993; Suh et al., 2001a). Efforts have also been made toward developing numerical models for predicting the

reflection coefficient (Kondo, 1979; Kakuno et al., 1992; Bennett et al., 1992; Fugazza and Natale, 1992; Suh and Park, 1995; Suh et al., 2001a). All the aforementioned studies dealt with the case in which a fully-perforated-wall caisson lies on a flat sea bed, except Park et al. (1993) and Suh and Park (1995). The former carried out a laboratory experiment of wave reflection from a partially-perforated-wall caisson mounted on a rubble foundation, while the latter developed a numerical model that predicts the wave reflection from a fully-perforated-wall caisson mounted on a rubble foundation. Both used only regular waves. Recently, on the other hand, Suh et al. (2002) compared the regular wave approximation and spectral wave approximation to compute the reflection of irregular waves from a perforated-wall caisson breakwater. They concluded that the spectral wave approximation is more adequate but the root-mean-squared wave height should be used for all the component waves to compute the energy dissipation at the perforated wall.

In the present paper, the experimental data of Park et al. (1993) are compared with Suh and Park's (1995) numerical model results. The Suh and Park's model, originally developed for a fully-perforated-wall caisson breakwater, is used for a partially-perforated-wall caisson breakwater by assuming that the lower part of the front face of the caisson (below the perforated wall), which is actually vertical, is assumed to have a very steep slope. In addition, a laboratory experiment is performed for irregular wave reflection from a partially-perforated-wall caisson breakwater using the same breakwater model as that used in the experiment of Park et al. (1993) for regular waves. Suh and Park's (1995) regular wave model is then applied, by following the method of Suh et al. (2002), to the calculation of irregular wave reflection. In the following section, the numerical model of Suh and Park (1995) and its extension to irregular waves (Suh et

al., 2002) are briefly described for the sake of completeness of the paper, although they were already published in the previous papers. In section 3, the experimental data for a partially-perforated-wall caisson subject to regular waves of Park et al. (1993) are compared with the numerical model. In section 4, the laboratory experiment for irregular waves is described. In section 5, the experimental results for irregular waves are compared with the predictions by the regular wave model. The major conclusions then follow.

2. Numerical model

Based on the extended refraction-diffraction equation proposed by Massel (1993), Suh and Park (1995) developed a numerical model to compute the reflection coefficient of a fully-perforated-wall caisson mounted on a rubble foundation when waves are obliquely incident to the breakwater at an arbitrary angle. The x-axis and y-axis are taken to be normal and parallel, respectively, to the breakwater crest line, and the water depth is assumed to be constant in y-direction. Taking $x = 0$ at the perforated wall, $x = -b$ at the toe of the rubble mound, and $x = B$ at the back wall of the wave chamber, Suh and Park (1995) showed that the function $\tilde{\varphi}(x)$ [see Suh and Park (1995) for its definition] on the rubble mound ($-b \le x \le 0$) satisfies the following ordinary differential equation:

$$\frac{d^2\tilde{\varphi}}{dx^2} + D(x)\frac{d\tilde{\varphi}}{dx} + E(x)\tilde{\varphi} = 0 \tag{1}$$

with the boundary conditions as follows:

$$\frac{d\tilde{\varphi}(-b)}{dx} = i[2-\tilde{\varphi}(-b)]k_1 \cos\theta_1 \tag{2}$$

$$\tilde{\varphi}(0) = \left[\frac{1}{\beta_3}\frac{\exp(-\beta_3 B)+\exp(\beta_3 B)}{\exp(-\beta_3 B)-\exp(\beta_3 B)} - \ell - \frac{i\gamma}{\omega}\right]\frac{d\tilde{\varphi}(0)}{dx} \tag{3}$$

The subscripts 1 and 3 denote the area of flat sea bed ($x \le -b$) and inside the wave chamber ($0 \le x \le B$), respectively, and θ is the wave incident angle. In (1), the depth-dependent functions $D(x)$ and $E(x)$ are given by

$$D(x) = \frac{k}{\tau + kh(1-\tau^2)}\left[1-3\tau^2 + \frac{2\tau}{\tau + kh(1-\tau^2)}\right]\frac{dh}{dx} \tag{4}$$

$$E(x) = k^2\left[1 + \frac{u_1}{k^2 u_0}\left(\frac{dh}{dx}\right)^2 + \frac{u_2}{k^2 u_0}\frac{d^2h}{dx^2}\right] - \chi^2 \tag{5}$$

where $\tau = \tanh(kh)$, k is the wave number which is related to the water depth h, wave angular frequency ω, and gravity g, by the dispersion relationship $\omega^2 = gk\tanh(kh)$, $\chi = k_1 \sin\theta_1 (= k_3 \sin\theta_3)$, and u_0, u_1, and u_2 are given by

$$u_0 = \frac{1}{2k}\tanh(kh)\left[1 + \frac{K}{\sinh K}\right] \tag{6}$$

$$u_1 = \frac{\mathrm{sech}^2(kh)}{4(K+\sinh K)}(\sinh K - K\cosh K) \tag{7}$$

$$\begin{aligned} u_2 = {} & \frac{k\,\mathrm{sech}^2(kh)}{12(K+\sinh K)^3}[K^4 + 4K^3\sinh K - 9\sinh K\sinh(2K) \\ & + 3K(K+2\sinh K)(\cosh^2 K - 2\cosh K + 3)] \end{aligned} \tag{8}$$

where the abbreviation $K = 2kh$ was used. As seen in (5), the model equation includes the terms proportional to the square of bottom slope and to the bottom curvature which were neglected in the mild-slope equation so that it can be applied over a bathymetry having substantial variation of water depth. Note that the coefficients associated with the higher-order bottom effect terms in Suh and Park's (1995) paper were replaced by those of Chamberlain and Porter (1995), which are given in more compact forms as in (6) to (8).

In (2) and (3), $i = \sqrt{-1}$, $\beta_3 = ik_3 \cos\theta_3$, ℓ is the length of the jet flowing through the perforated wall, and γ is the linearized dissipation coefficient at the perforated wall given by (Fugazza and Natale, 1992)

$$\gamma = \frac{8\alpha}{9\pi} H_w \omega \frac{W}{\sqrt{W^2(R+1)^2 + G^2}} \frac{5 + \cosh(2k_3h_3)}{2k_3h_3 + \sinh(2k_3h_3)} \tag{9}$$

where H_w is the incident wave height at the perforated wall, $W = \tan(k_3 B)$, $R = \gamma k_3 / \omega$, $G = 1 - PW$, $P = \ell k_3$, and α is the energy loss coefficient at the perforated wall:

$$\alpha = \left(\frac{1}{r \cos\theta_3 C_c} \right)^2 - 1 \tag{10}$$

where r is the porosity of the perforated wall. In the preceding equation, $r\cos\theta_3$ denotes the effective ratio of the opening of the perforated wall taking into account the

oblique incidence of the waves to the wall. For normal incidence, this reduces to r as in Fugazza and Natale (1992). C_c is the empirical contraction coefficient at the perforated wall. Mei et al. (1974) suggest using the formula

$$C_c = 0.6 + 0.4r^2 \tag{11}$$

for a rectangular geometry like a vertical slit wall. Note that R in Eq. (9) is a function of γ. Rearranging (9) gives a quartic polynomial of γ, which can be solved by the eigenvalue method [see Press et al. (1992), p. 368].

In (3), the jet length, ℓ, represents the inertial resistance at the perforated wall. Fugazza and Natale (1992) assumed that the importance of the local inertia term is weak, and they took the jet length to be equal to the wall thickness, d. On the other hand, Kakuno and Liu (1993) proposed a blockage coefficient to represent the inertial resistance of a vertical slit wall:

$$C = \frac{d}{2}\left(\frac{A}{a} - 1\right) + \frac{2A}{\pi}\left[1 - \log\left(\frac{4a}{A}\right) + \frac{1}{3}\left(\frac{a}{A}\right)^2 + \frac{281}{180}\left(\frac{a}{A}\right)^4\right] \tag{12}$$

where $2A$ is the center-to-center distance between two adjacent members of the slit wall, $2a$ is the width of a slit, so that the porosity of the wall is $r = a/A$. By comparing the Fugazza and Natale (1992) and Kakuno and Liu (1993) models, Suh et al. (2002) showed that

$$\ell = 2C \tag{13}$$

which is much greater than the wall thickness, d, implying the influence of the inertial resistance term is not so insignificant. In this study, (12) and (13) were used to calculate the jet length.

The differential equation (1) with the boundary conditions (2) and (3) can be solved using a finite difference method. Using the forward-differencing for $d\tilde{\varphi}(-b)/dx$, backward-differencing for $d\tilde{\varphi}(0)/dx$, and central-differencing for the derivatives in (1), the boundary value problem (1) to (3) is approximated by a system of linear equations, $\mathbf{AY} = \mathbf{B}$, where $\mathbf{A}$ is a tridiagonal band type matrix, $\mathbf{Y}$ is a column vector, and $\mathbf{B}$ is also a column vector. After solving this matrix equation, the reflection coefficient C_r is calculated by

$$C_r = \mathrm{Re}\{\tilde{\varphi}(-b) - 1\} \tag{14}$$

where the symbol Re represents the real part of a complex value.

In the calculation of the dissipation coefficient γ in (9), the incident wave height at the perforated wall H_w is a priori unknown. In the case where the caisson does not exist and the water depth is constant as h_3 for $x \geq 0$ (Note that h_3 is not the water depth inside the wave chamber but that on the rubble mound berm in the case of a partially-perforated-wall caisson breakwater), Massel (1993) has shown that the transmitting boundary condition at $x = 0$ is given by

$$i\tilde{\varphi}(0)k_3 \cos\theta_3 = \frac{d\tilde{\varphi}(0)}{dx} \tag{15}$$

The governing equation (1) and the upwave boundary condition (2) do not change. After solving this problem, the transmission coefficient C_t is given by $C_t = \mathrm{Re}\{\tilde{\varphi}(0)\}$, from which H_w is calculated as C_t times the incident wave height on the flat bottom.

As for irregular waves, the reflection coefficient is calculated differently for each frequency component. The wave period is determined according to the frequency of the component wave, while the root-mean-squared wave height is used for all the component waves to compute the energy dissipation at the perforated wall. The spectral density of the reflected waves is calculated for a particular frequency component by

$$S_{\eta,r}(f) = |C_r(f)|^2 S_{\eta,i}(f) \tag{16}$$

where f is the wave frequency and $S_{\eta,i}(f)$ is the incident wave energy spectrum. The frequency-averaged reflection coefficient is then calculated as (Goda, 2000)

$$\overline{C_r} = \sqrt{\frac{m_{0,r}}{m_{0,i}}} \tag{17}$$

where $m_{0,i}$ and $m_{0,r}$ are the zeroth moments of the incident and reflected wave spectra, respectively, obtained by integrating each spectrum over the entire frequency range.

3. Comparison with experimental data for regular waves

Park et al. (1993) carried out a laboratory experiment in the wave flume at Korea Ocean Research and Development Institute, which was 53.15 m long, 1 m wide, and 1.25 m high. A composite breakwater with a partially-perforated-wall caisson was used in the experiment. Fig. 2 shows an example of the breakwater model with a wave chamber width of 20 cm. The mound was constructed with crushed stones of 0.12 to 0.24 cm^3 class and it was covered by thick armor stones of 5.6 cm^3 class. Two rows of concrete blocks of 3 cm thickness were put at the front and back of the caisson. The total height of the mound was 24 cm with 1:2 fore and back slopes, and the berm width of the mound was 25 cm. The model caisson was made of transparent acrylic plates of 10 mm thickness. Park et al. (1993) used three different types of perforated walls of the same porosity but with vertical slits, horizontal slits, or circular holes. They found that the difference of reflection coefficients of different types of perforated walls was small. In this study, only the data of the vertical slit wall are used, which contained vertical slits of 2 cm width and 27 cm height with 4 cm separation between each slit so that the wall porosity was 0.33. The breakwater model was installed at a distance of about 30 m from the wavemaker. Wave measurements were made in the middle between the wavemaker and the breakwater by three wave gauges separated by 20 and 35 cm one another along the flume. The method of Park et al. (1992) was then used to separate the incident and reflected waves.

The water depths on the flat bottom, on the berm and inside the wave chamber were 50, 26 and 17 cm, respectively. The crest elevation of the caisson was 12 cm above the still water level, thus excluding any wave overtopping for all tests. Regular waves were generated. The wave period was changed from 0.7 to 1.8 s at the interval of 0.1 s, and two different wave heights of 5 and 10 cm were used for each wave period, except 0.7

and 0.8 s wave periods for which only 5 cm wave height was used. Three different wave chamber widths of 15, 20, and 25 cm were used. This resulted in a total of 66 test cases.

It is well known that the wave reflection from a perforated-wall caisson breakwater depends on the width of the wave chamber relative to the wavelength. For a fully-perforated-wall caisson lying on a flat sea bed, Fugazza and Natale (1992) showed that the resonance inside the wave chamber is important so that the reflection is at its minimum when $B/L = 0.25$ where B is the wave chamber width and L is the wavelength. For a fully-perforated-wall caisson lying on a flat bed, the wavelength does not change as the wave propagates into the wave chamber as long as the inertia resistance at the perforated wall is assumed to be negligible. For a partially-perforated-wall caisson mounted on a rubble mound which is examined in this study, however, the wavelength changes as the wave propagates from the flat bottom to the wave chamber. Since the wave reflection of a perforated-wall caisson is related to the resonance inside the wave chamber, it may be reasonable to examine the reflection coefficient as a function of the wave chamber width normalized with respect to the wavelength inside the wave chamber.

Fig. 3 shows the variation of the measured reflection coefficients with respect to B/L_c where L_c is the wavelength inside the wave chamber. The reflection coefficient shows its minimum at B/L_c around 0.2, which is somewhat smaller than the theoretical value of 0.25 obtained by Fugazza and Natale (1992). In the analysis of Fugazza and Natale, they neglected the inertia resistance at the perforated wall. In front of a perforated-wall caisson breakwater, a partial standing wave is formed due to the wave reflection from the breakwater. If there were no perforated wall, the node would occur at a distance of $L_c/4$ from the back wall of the wave chamber, and hence the

largest energy loss would occur at this distance. In reality, however, due to the inertia resistance at the perforated wall, a phase differences occur between inside and outside of the wave chamber in such a way that the perforated wall slows the waves. Consequently the location of the node will move onshore, and the distance where the largest energy loss is gained becomes smaller than $L_c/4$. Therefore, the minimum reflection occurs at a value of B/L_c smaller than 0.25. In Fig. 3, it is also seen that increasing wave steepness leads to a reduction in the reflection coefficient. This is associated with an increase in the energy dissipation within the breakwater at higher wave steepnesses.

The numerical model described in the previous section assumes that the water depth inside the wave chamber is the same as that on the mound berm as in a fully-perforated-wall caisson breakwater shown in Fig. 1(a). However, for a partially-perforated-wall caisson breakwater used in the experiment (see Fig. 2), these water depths are different each other, having depth discontinuity at the location of the perforated wall. In order to apply the model to the case of a partially-perforated-wall caisson, we assume that the lower part of the front face of the caisson (below the perforated wall) is not vertical but has a very steep slope. As mentioned previously, the model equation (1), which includes the terms proportional to the square of bottom slope and to the bottom curvature, can be applied over a bed having substantial variation of water depth. In order to examine the effect of the slope of the lower part of the caisson (which is infinity in reality), the reflection coefficient was calculated by changing the slope from 0.1 to 10 for the test of wave period of 1.3 s, wave height of 5 cm, and wave chamber width of 20 cm, in which the measured reflection coefficient was 0.33. Fig. 4 shows the calculated reflection coefficients for different slopes of the lower part of the caisson. The reflection

coefficient virtually does not change for slopes greater than 2.0. In the following calculations, the slope was fixed at 4.0.

Fig. 5 shows a comparison between the measured and calculated reflection coefficients. In this figure, the open and solid symbols denote the incident wave height of 5 and 10 cm, respectively. The data of the smaller wave height show reasonable agreement between measurement and calculation, though the numerical model slightly over-predicts the reflection coefficients at larger C_r values and under-predicts them at smaller C_r values probably because the evanescent waves near the breakwater were neglected (see Suh et al. 2001a). For the data of the larger wave height, the model significantly over-predicts the reflection coefficient when the reflection coefficients are small. The present model is based on a linear wave theory and it utilizes the linearized energy dissipation coefficient at the perforated wall as in (9). Therefore, the model may not be applicable to highly nonlinear waves. In order to examine the effect of nonlinearity, the ratio of the calculated reflection coefficient to the measured one was plotted in Fig. 6 in terms of the wave steepness, H_0 / L_0, in which H_0 and L_0 are the deepwater wave height and wavelength, respectively. It is observed that the model tends to overestimate the reflection coefficient as the wave steepness increases. In Fig. 6, it is shown that the model gives reasonably accurate results for the deepwater wave steepness up to about 0.02. At this value, the deepwater wave height, H_0, for T = 6, 8, and 10 s is approximately 1, 2, and 3 m, respectively. Considering that the wave reflection from a breakwater is of more interest for ordinary waves than the severe storm waves (because most ships seek refuge into harbors during the severe wave condition), the present model may provide useful information about wave reflection in the design of perforated-wall caisson breakwaters. Also note that the agreement between

measurement and calculation is good for the reflection coefficients greater than about 0.3 (see Fig. 5). This fact supports the usefulness of the numerical model because larger reflection coefficients may be of more interest in the design of breakwaters, for which the model is more error-free.

4. Laboratory experiment for irregular waves and comparison with numerical model prediction

In order to examine the applicability of the regular wave model to irregular waves, laboratory experiments were conducted in the wave tank at the Coastal Engineering Laboratory of Seoul National University. The wave tank was 11 m wide, 23 m long, and 1 m high. The wave paddle was only 6 m wide, so guide walls were installed along the tank and wave absorbers at both ends of the tank as shown in Fig. 7. Inside these guide walls, another pair of guide walls of 1 m separation was installed to accommodate the breakwater model. The breakwater model and the water depth were the same as those used in the experiment of Park et al. (1993) (See Fig. 2). Waves were generated with a piston-type wavemaker. Water surface displacements were measured with parallel-wire capacitance-type wave gauges.

To measure the incident and reflected wave spectra, three wave gauges were installed inside the inner guide walls, as shown in Fig. 7. The free surface displacements measured by these wave gauges were used to separate the incident and reflected wave spectra using the method of Suh et al. (2001b). For the purpose of cross-check, the incident waves were also measured at a point outside the guide walls denoted as G4 in Fig. 7, where the effect of wave reflection from the breakwater is minimal. Wave

measurements were made for 300 s at a sampling rate of 20 Hz at each of the wave gauges. For spectral analysis, the last 4096 data were used. The time series was corrected by applying a 10% cosine taper on both ends and was subjected to spectral analysis. The raw spectrum was running-averaged twice over 15 neighboring frequency bands, the total number of degrees of freedom of the final estimates being 225.

The incident wave spectrum used in the experiment was the Bretschneider-Mitsuyasu spectrum given by

$$S_{\eta,i}(f) = 0.205 H_s^2 T_s (T_s f)^{-5} \exp[-0.75(T_s f)^{-4}] \tag{18}$$

where H_s and T_s are the significant wave height and period, respectively. The target significant wave heights and periods are given in Table 1 with other experimental conditions and calculated parameters. Similarly to the experiment of Park et al. (1993), the significant wave period was changed from 1.1 to 2.0 s at the interval of 0.1 s, and two different significant wave heights of 5 and 10 cm were used for each wave period, except 1.1 and 1.2 s wave periods for which only 5 cm wave height was used. These wave conditions were used for three different wave chamber widths of 15, 20, and 25 cm, resulting in a total of 54 test cases. The error of the model prediction was calculated by

$$\text{Error} = \frac{\overline{C}_r^c - \overline{C}_r^m}{\overline{C}_r^c} \times 100\% \tag{19}$$

where the superscripts c and m indicate calculation and measurement, respectively.

Fig. 8 shows the variation of the measured frequency-averaged reflection coefficients with respect to B/L_{cs} where L_{cs} is the significant wavelength inside the wave chamber. The data do not cover the range of B/L_{cs} larger than 0.18, but their trend shows that the minimum reflection would occur at B/L_{cs} close to 0.2, as with regular waves. While the minimum reflection coefficient was as small as almost zero for regular waves (see Fig. 3), it lies between 0.3 and 0.4 for irregular waves. This agrees with the experimental results reported by Tanimoto et al. (1976) and Suh et al. (2001a) for fully-perforated-wall caisson breakwaters. The reflection coefficient is different for each frequency in irregular waves. Even though the reflection coefficient is almost zero at a certain frequency, it is large at other frequencies. Therefore, the frequency-averaged reflection coefficient of irregular waves cannot be very small. Again as with regular waves, increasing wave steepness leads to a reduction in the reflection coefficient, because of the increase in the energy dissipation within the breakwater at higher wave steepnesses.

Fig. 9 shows a comparison between the measured and calculated frequency-averaged reflection coefficients. The open and solid symbols denote the incident significant wave height of 5 and 10 cm, respectively. A reasonable agreement is shown between measurement and calculation, but, as with regular waves, the numerical model somewhat over-predicts the reflection coefficients at larger values and under-predicts them at smaller values because the evanescent waves near the breakwater were neglected. The significant over-prediction of the reflection coefficient observed in the case of highly nonlinear regular waves is not observed in the case of irregular waves.

Finally, we present comparisons of the measured and calculated spectra of reflected waves for several cases. Fig. 10 shows the results for the case of H_s = 10 cm, T_s =

1.9 s and B = 25 cm, for which the error for the frequency-averaged reflection coefficient was the smallest as -0.6%. Note that the measured incident wave spectrum was used to calculate the reflected wave spectrum. A good agreement is shown between measurement and calculation, though the numerical model slightly over-predicts the wave reflection near the peak frequency and under-predicts it at higher frequencies. Fig. 11 shows the results for the case of H_s = 5 cm, T_s = 1.1 s, and B = 25 cm, for which the error for the frequency-averaged reflection coefficient was the largest as -35.3%. The numerical model under-predicts the wave reflection throughout the frequency, but the overall agreement is still acceptable. Similar plots for other test conditions can be found in Park (2004).

5. Conclusions

In this study, we examined the use of the numerical model of Suh and Park (1995), which was developed to predict the reflection of regular waves from a fully-perforated-wall caisson breakwater, for predicting the regular or irregular wave reflection from a partially-perforated-wall caisson breakwater. For this we assumed that the lower part of the front face of the partially-perforated-wall caisson is not vertical but has a very steep slope. A numerical test carried out by changing this slope and the comparison of the model prediction with the experimental data of Park et al. (1993) showed that such an assumption was reasonable and that the Suh and Park's model can be used for predicting the regular wave reflection from a partially-perforated-wall caisson breakwater. The Suh and Park's regular wave model was then used for computing the irregular wave reflection by following the method of Suh et al. (2002), in which the wave period was

determined according to the frequency of the component wave, while the root-mean-squared wave height was used for all the component waves to compute the energy dissipation at the perforated wall. A laboratory experiment was carried out to examine the validity of the model for irregular wave reflection. Reasonable agreements were observed between measurement and prediction for both frequency-averaged reflection coefficients and reflected wave spectra.

For regular and irregular waves, respectively, the reflection coefficient showed its minimum when B/L_c and B/L_{cs} are approximately 0.2. While the minimum reflection coefficient was as small as almost zero for regular waves, it lay between 0.3 and 0.4 for irregular waves. Increasing wave steepness led to a reduction in the reflection coefficient due to the increase in the energy dissipation within the breakwater at higher wave steepnesses. It was shown that the numerical model based on a linear wave theory tends to over-predict the reflection coefficient of regular waves as the wave nonlinearity increases. However, such an over-prediction was not observed in the case of irregular waves. For both regular and irregular waves, the numerical model slightly over-predicted the reflection coefficients at larger values, and under-predicted at smaller values because the model neglected the evanescent waves near the breakwater.

Acknowledgement

KDS and JKP were supported by the Brain Korea 21 Project.

References

Bennett, G.S., McIver, P., Smallman, J.V., 1992. A mathematical model of a slotted wavescreen breakwater. Coastal Engineering 18, 231-249.

Chamberlain, P.G., Porter, D., 1995. The modified mild-slope equation. Journal of Fluid Mechanics 291, 393-407.

Fugazza, M., Natale, L., 1992. Hydraulic design of perforated breakwaters. Journal of Waterway, Port, Coastal and Ocean Engineering 118(1), 1-14.

Goda, Y., 2000. Random Seas and Design of Maritime Structures, 2nd edn. World Scientific, Singapore, 443 pp.

Jarlan, G.E., 1961. A perforated vertical wall breakwater. The Dock & Harbour Authority XII (486), 394-398.

Kakuno, S., Liu, P.L.-F., 1993. Scattering of water waves by vertical cylinders. Journal of Waterway, Port, Coastal and Ocean Engineering 119(3), 302-322.

Kakuno, S., Oda, K., Liu, P.L.-F., 1992. Scattering of water waves by vertical cylinders with a backwall. Proc. 23rd Int. Conf. on Coastal Engineering, ASCE, Venice, Italy, vol. 2, pp. 1258-1271.

Kondo, H., 1979. Analysis of breakwaters having two porous walls. Proc. Coastal Structures ’79, ASCE, vol. 2, pp. 962-977.

Marks, M., Jarlan, G.E., 1968. Experimental study on a fixed perforated breakwater. Proc. 11th Int. Conf. on Coastal Engineering, ASCE, London, UK, vol. 3, pp. 1121-1140.

Massel, S.R., 1993. Extended refraction-diffraction equation for surface waves. Coastal Engineering 19, 97-126.

Mei, C.C., Liu, P.L.-F., Ippen, A.T., 1974. Quadratic loss and scattering of long waves. Journal of Waterway, Harbors and Coastal Engineering Division, ASCE 100, 217-

239.

Park, J.K., 2004. Irregular wave reflection from partially perforated caisson breakwater. Master thesis, Seoul National University, Seoul, Korea (in Korean).

Park, W.S., Chun, I.S., Lee, D.S., 1993. Hydraulic experiments for the reflection characteristics of perforated breakwaters. Journal of Korean Society of Coastal and Ocean Engineers 5(3), 198-203 (in Korean, with English abstract).

Park, W.S., Oh, Y.M., Chun, I.S., 1992. Separation technique of incident and reflected waves using least squares method. Journal of Korean Society of Coastal and Ocean Engineers 4(3), 139-145 (in Korean, with English abstract).

Press, W.H., Teukolsky, S.A., Vetterling, W.T., Flannery, B.P., 1992. Numerical Recipes in FORTRAN: The Art of Scientific Computing, 2nd edn. Cambridge University Press, 963 pp.

Suh, K.D., Choi, J.C., Kim, B.H., Park, W.S., Lee, K.S., 2001a. Reflection of irregular waves from perforated-wall caisson breakwaters. Coastal Engineering 44, 141-151.

Suh, K.D., Park, W.S., 1995. Wave reflection from perforated-wall caisson breakwaters. Coastal Engineering 26, 177-193.

Suh, K.D., Park, W.S., Park, B.S., 2001b. Separation of incident and reflected waves in wave-current flumes. Coastal Engineering 43, 149-159.

Suh, K.D., Son, S.Y., Lee, J.I., Lee, T.H., 2002. Calculation of irregular wave reflection from perforated-wall caisson breakwaters using a regular model. Proc. 28th Int. Conf. on Coastal Engineering, ASCE, Cardiff, UK, vol. 2, pp. 1709-1721.

Takahashi, S., Shimosako, K., 1994. Wave pressure on a perforated caisson. Proc. Hydro-Port ’94, Port and Harbour Research Institute, Yokosuka, Japan, vol. 1, pp. 747-764.

Takahashi, S., Tanimoto, K., Shimosako, K., 1994. A proposal of impulsive pressure coefficient for the design of composite breakwaters. Proc. Hydro-Port ’94, Port and Harbour Research Institute, Yokosuka, Japan, vol. 1, pp. 489-504.

Tanimoto, K., Haranaka, S., Takahashi, S., Komatsu, K., Todoroki, M., Osato, M., 1976. An experimental investigation of wave reflection, overtopping and wave forces for several types of breakwaters and sea walls. Tech. Note of Port and Harbour Res. Inst., Ministry of Transport, Japan, No. 246, 38 pp. (in Japanese, with English abstract).

Terret, F.L., Osorio, J.D.C., Lean, G.H., 1968. Model studies of a perforated breakwater. Proc. 11th Int. Conf. on Coastal Engineering, ASCE, London, UK, vol. 3, pp. 1104-1120.

Table 1 Experimental conditions and analyzed data

B (cm)	H_s (cm)	T_s (s)	H_s^m (cm)	T_s^m (s)	$\overline{C}_r^c$	$\overline{C}_r^m$	Error(%)
15	5	1.1	5.14	1.24	0.489	0.506	−3.4
	5	1.2	4.99	1.33	0.555	0.561	−1.1
	5	1.3	4.94	1.40	0.593	0.559	5.8
	5	1.4	4.75	1.49	0.645	0.573	11.2
	5	1.5	5.08	1.55	0.660	0.591	10.6
	5	1.6	4.99	1.63	0.707	0.631	10.7
	5	1.7	4.89	1.73	0.752	0.673	10.5
	5	1.8	4.67	1.83	0.787	0.707	10.2
	5	1.9	4.79	1.86	0.801	0.741	7.5
	5	2.0	4.88	1.97	0.825	0.756	8.3
	10	1.3	9.43	1.41	0.513	0.488	4.9
	10	1.4	9.40	1.47	0.545	0.493	9.5
	10	1.5	9.63	1.54	0.573	0.528	8.0
	10	1.6	9.60	1.68	0.624	0.551	11.6
	10	1.7	9.82	1.83	0.674	0.599	11.2
	10	1.8	9.49	1.88	0.708	0.646	8.8
	10	1.9	10.08	1.90	0.717	0.668	6.9
	10	2.0	9.11	2.07	0.774	0.681	12.0
20	5	1.1	5.25	1.23	0.366	0.453	−23.7
	5	1.2	5.09	1.32	0.409	0.481	−17.8
	5	1.3	5.10	1.39	0.440	0.492	−11.8
	5	1.4	5.03	1.49	0.476	0.493	−3.5
	5	1.5	5.31	1.54	0.502	0.539	−7.3
	5	1.6	5.20	1.62	0.556	0.550	1.2
	5	1.7	5.00	1.66	0.599	0.586	2.2
	5	1.8	4.75	1.75	0.641	0.596	7.0
	5	1.9	5.32	1.78	0.640	0.598	6.6
	5	2.0	4.69	1.77	0.691	0.667	3.4
	10	1.3	9.76	1.38	0.378	0.411	−8.7
	10	1.4	9.89	1.44	0.398	0.423	−6.2
	10	1.5	10.16	1.53	0.433	0.427	1.3
	10	1.6	9.17	1.61	0.505	0.484	4.0
	10	1.7	9.13	1.73	0.545	0.525	3.7
	10	1.8	10.02	1.88	0.556	0.524	5.9
	10	1.9	10.57	1.94	0.586	0.524	10.5
	10	2.0	8.96	1.94	0.627	0.585	6.8

Table 1 (Continued)

B (cm)	H_s (cm)	T_s (s)	H_s^m (cm)	T_s^m (s)	$\overline{C}_r^c$	$\overline{C}_r^m$	Error(%)
25	5	1.1	5.27	1.23	0.335	0.454	–35.3
	5	1.2	4.97	1.28	0.378	0.481	–27.4
	5	1.3	5.17	1.35	0.372	0.474	–27.4
	5	1.4	4.65	1.45	0.386	0.484	–25.3
	5	1.5	5.25	1.53	0.377	0.488	–29.5
	5	1.6	4.88	1.51	0.476	0.535	–12.4
	5	1.7	5.07	1.68	0.459	0.513	–11.6
	5	1.8	4.94	1.76	0.509	0.551	–8.2
	5	1.9	5.36	1.78	0.511	0.550	–7.6
	5	2.0	4.55	1.87	0.607	0.589	3.0
	10	1.3	9.58	1.37	0.320	0.395	–23.4
	10	1.4	9.67	1.42	0.337	0.395	–17.1
	10	1.5	9.79	1.51	0.349	0.406	–16.3
	10	1.6	9.83	1.60	0.387	0.435	–12.4
	10	1.7	10.27	1.74	0.408	0.438	–7.3
	10	1.8	10.32	1.85	0.442	0.463	–4.8
	10	1.9	10.82	1.94	0.474	0.477	–0.6
	10	2.0	8.82	1.88	0.513	0.505	1.7

Caption of figures

1. Bird's-eye views of (a) a fully-perforated-wall caisson breakwater and (b) a partially-perforated-wall caisson breakwater.
2. Illustration of the breakwater model.
3. Variation of the measured reflection coefficients with respect to B/L_c (regular waves).
4. Reflection coefficients calculated for different slopes of the lower part of the caisson.
5. Comparison of the reflection coefficients between measurement and calculation for regular waves: ○ = wave height of 5 cm; ● = wave height of 10 cm.
6. Ratio of calculated reflection coefficient to measured one in terms of wave steepness.
7. Experimental setup for irregular wave reflection.
8. Variation of the measured frequency-averaged reflection coefficients with respect to B/L_{cs}.
9. Comparison of the frequency-averaged reflection coefficients between measurement and calculation: ○ = significant wave height of 5 cm; ● = significant wave height of 10 cm.
10. Measured and calculated spectra of incident and reflected waves for the case of H_s = 10 cm, T_s = 1.9 s, and B = 25 cm: thick solid line = measured incident wave, thick dash-dot line = target incident wave, thin solid line = measured reflected wave, thin dashed line = calculated reflected wave.
11. Same as Fig. 10, but for H_s = 5 cm, T_s = 1.1 s, and B = 25 cm.

Fig. 1. Bird's-eye views of (a) a fully-perforated-wall caisson breakwater and (b) a partially-perforated-wall caisson breakwater.

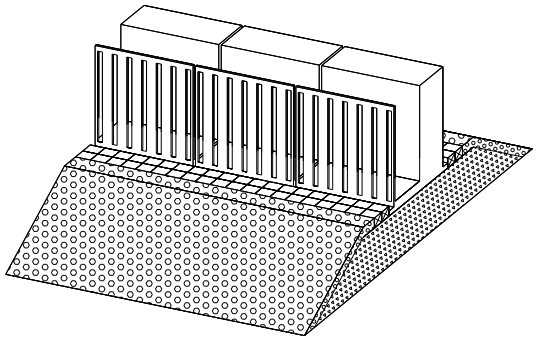

(a)

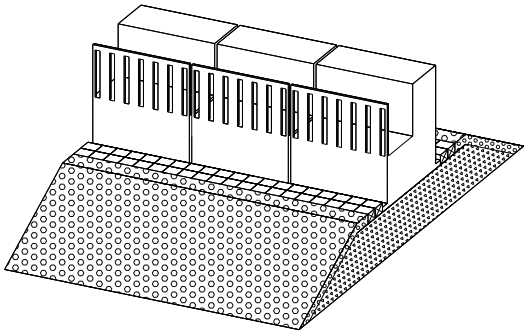

(b)

Fig. 2. Illustration of the breakwater model (unit: cm).

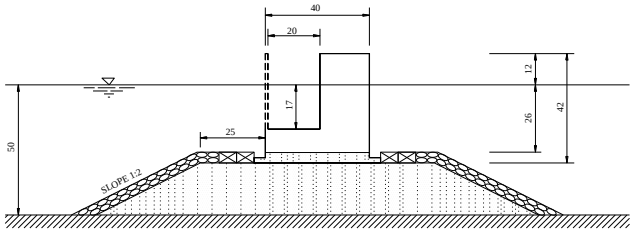

Fig. 3. Variation of the measured reflection coefficients with respect to B/L_c (regular waves).

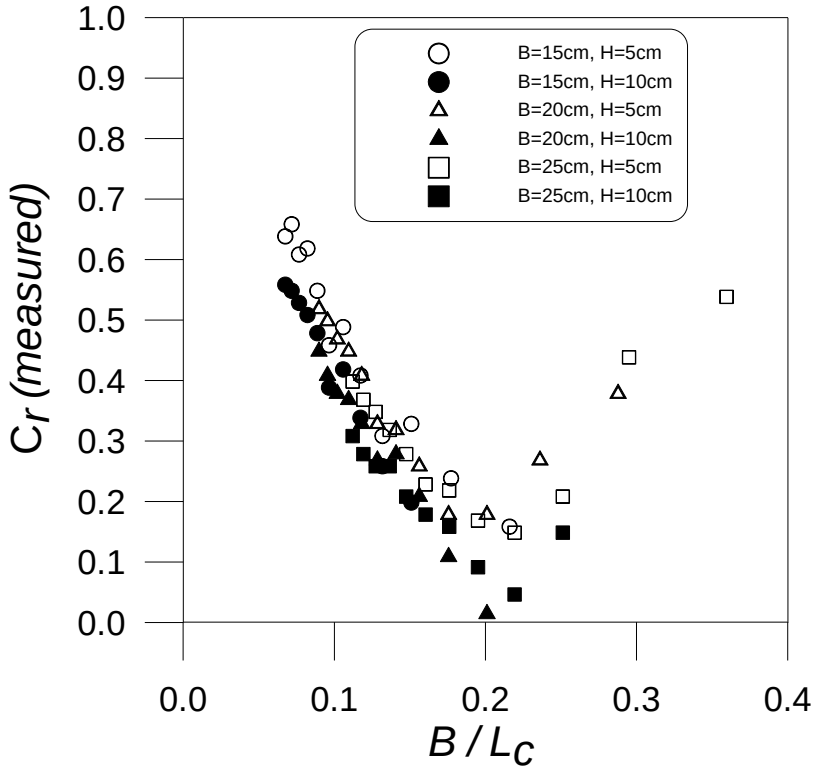

Fig. 4. Reflection coefficients calculated for different slopes of the lower part of the caisson.

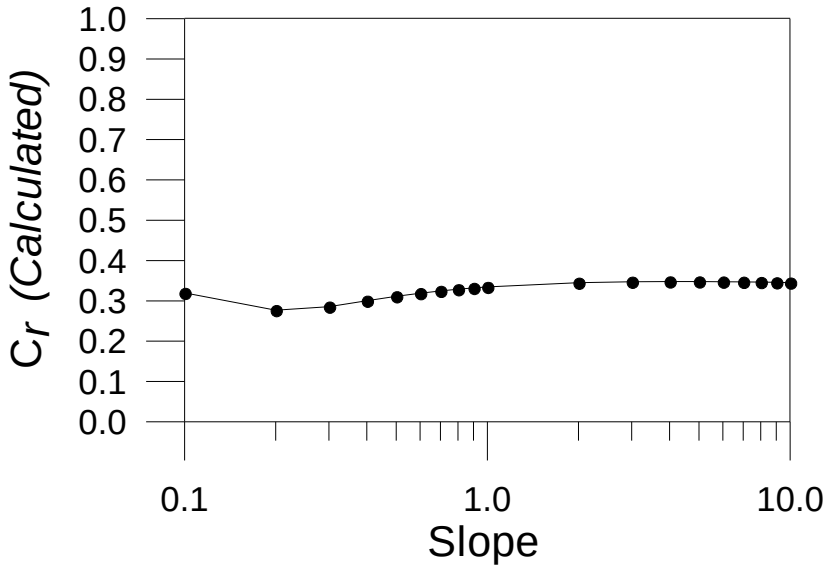

Fig. 5. Comparison of the reflection coefficients between measurement and calculation for regular waves: ○ = wave height of 5 cm; ● = wave height of 10 cm.

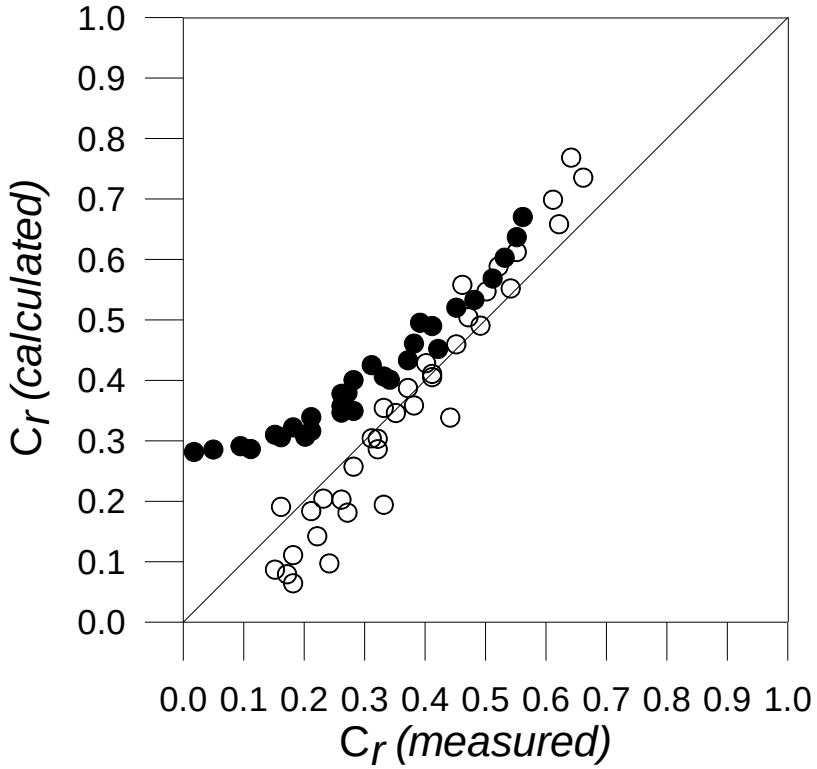

Fig. 6. Ratio of calculated reflection coefficient to measured one in terms of wave steepness.

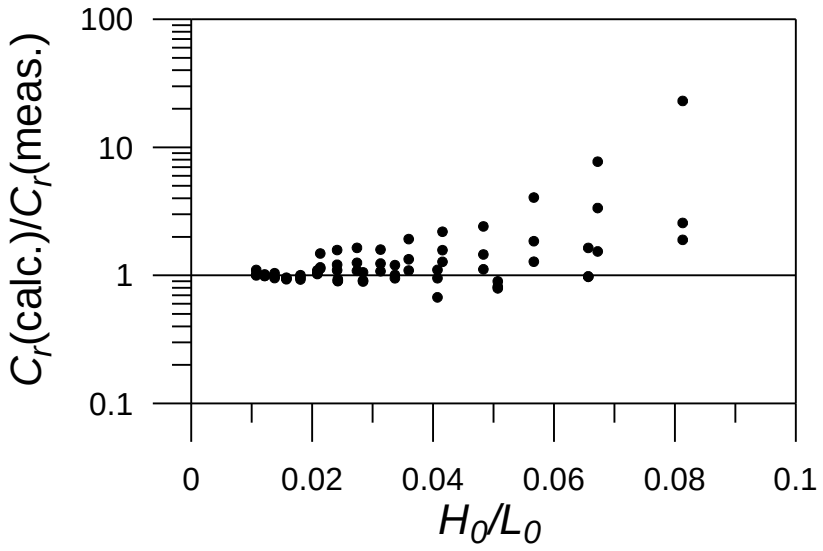

Fig. 7. Experimental setup for irregular wave reflection.

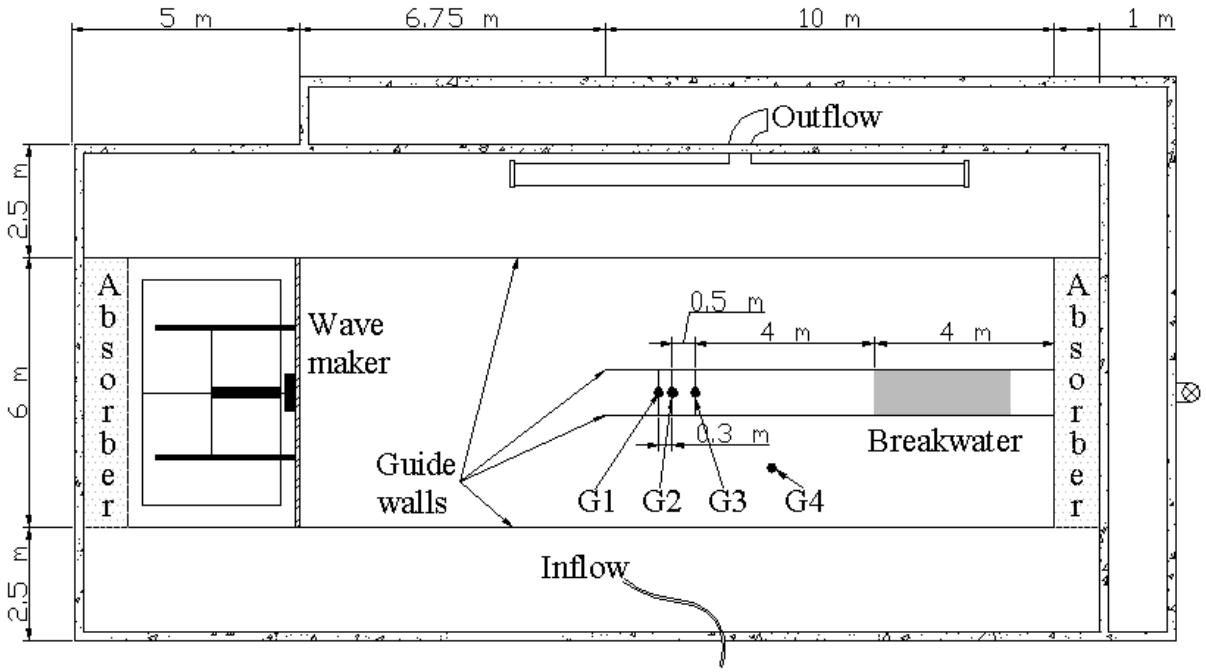

Fig. 8. Variation of the measured frequency-averaged reflection coefficients with respect to B/L_{cs}.

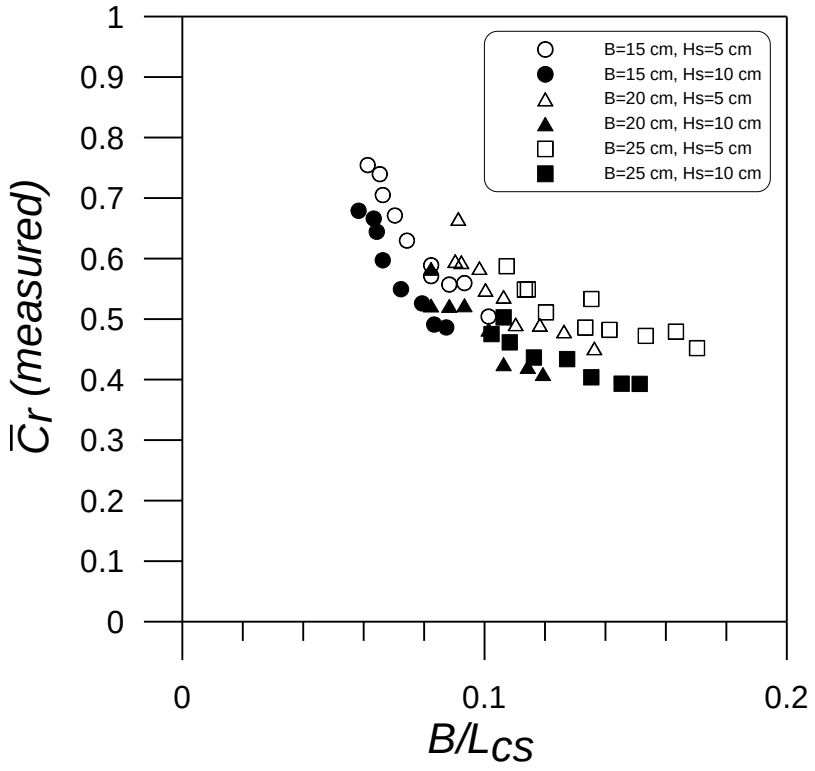

Fig. 9. Comparison of the frequency-averaged reflection coefficients between measurement and calculation: ○ = significant wave height of 5 cm; ● = significant wave height of 10 cm.

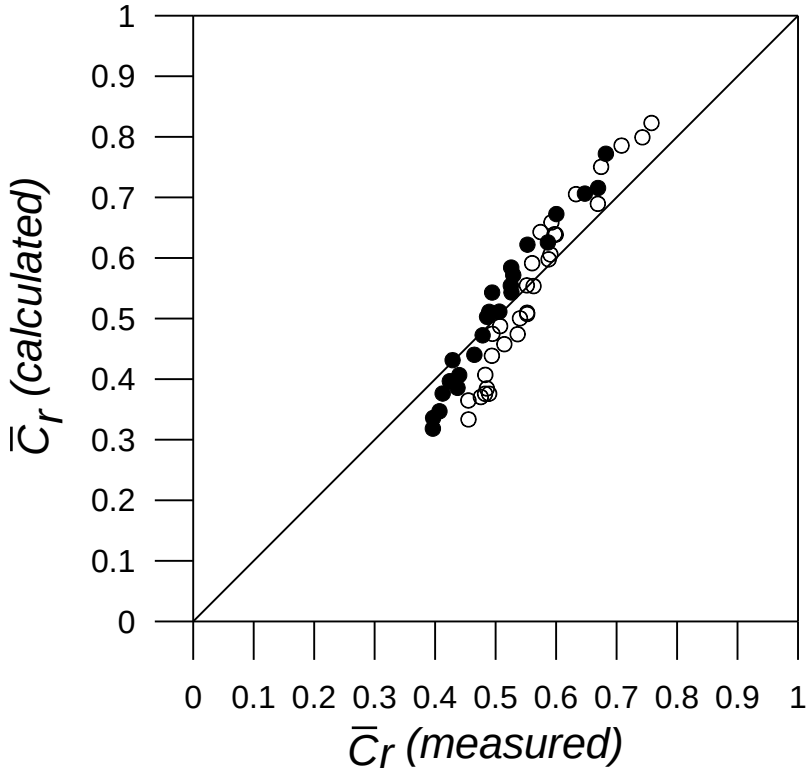

Fig. 10. Measured and calculated spectra of incident and reflected waves for the case of H_s = 10 cm, T_s = 1.9 s, and B = 25 cm: thick solid line = measured incident wave, thick dash-dot line = target incident wave, thin solid line = measured reflected wave, thin dashed line = calculated reflected wave.

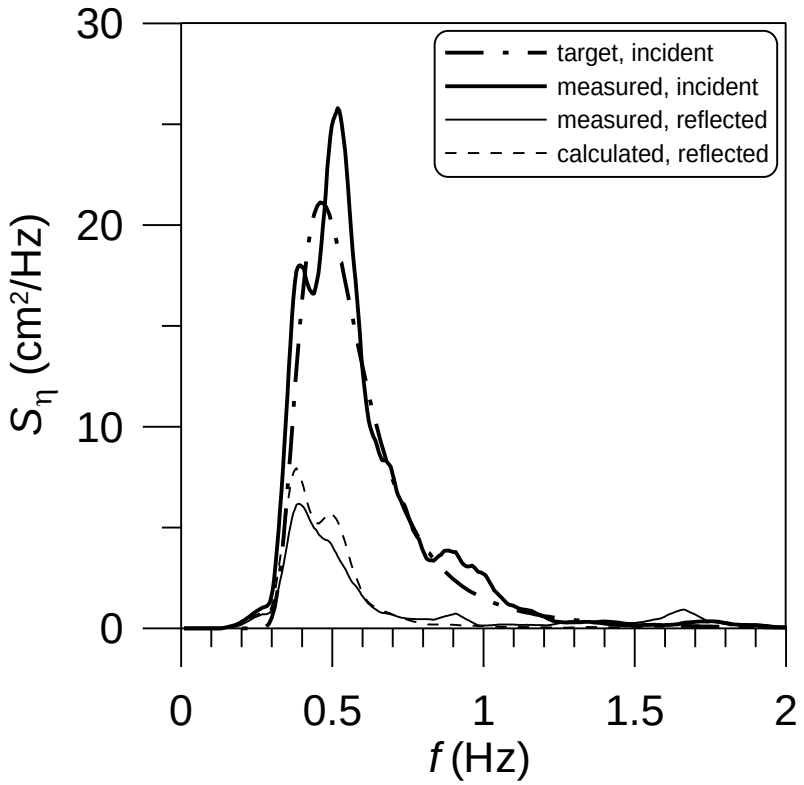

Fig. 11. Same as Fig. 10, but for H_s = 5 cm, T_s = 1.1 s, and B = 25 cm